Chapter

Nanoparticle Formation and Deposition by Pulsed Laser Ablation

Toshio Takiya and Naoaki Fukuda

Abstract

Pulsed Laser Ablation (PLA) in background gas is a good technique to acquire specific nanoparticles under strong non-equilibrium states. Here, after a history of PLA is mentioned, the application of nanoparticles and its deposition films to the several fields will be described. On the target surface heated with PLA, a Knudsen layer is formed around the adjacent region of the surface, and high-pressure and high-temperature vapor atoms are generated. The plume formed by evaporated atoms blasts off with very high-speed and expands rapidly with a shock wave. A supercooling phenomenon occurs during this process, and number of nucleus of nanoparticle forms in vapor-phase. The nuclei grow by the condensation of vapor atoms and deposit on a substrate as nanoparticle film. If the radius of nanoparticle is uniformized, a self-ordering formation can be shown as a result of interactive process between each nanoparticle of the same size on the substrate. In this chapter, the related technology to realize a series of these processes will be expounded.

Keywords: PLA, PLD, nanoparticle, deposition, non-equilibrium, evaporation, laser plume, shock wave

1. Introduction

Pulsed Laser Deposition (PLD), which is a film-forming technique by using PLA, has been experimented since the 1960s after the invention of the laser oscillator. Afterwards, in the wake of the realization of Q-switch Nd: YAG laser in 1970s and the electric discharge pumping high-speed repeatable excimer laser in 1980s, PLD has become a powerful tool to fabricate high-performance films such as semiconductors, heterostructure and superlattices. The success of high-temperature superconducting films in the mid-1980s led to the flourishing of laser ablation research.

In the early 1990s, the research on PLD application has made several developments such as heteroepitaxial films, perovskite oxide films, nitride films and diamond-like carbon films. Although the research on nanoparticles derived from the laser ablation had already been conducted as part of these developments, the discovery of Buckminster fullerene [1] was undoubtedly an important milestone in the following development of nanoparticle applications. In the 21st century, effect which shock waves have on the formation way of nanoparticle during laser ablation has been investigated [2, 3]. Several researches [4–6] in which the shock waves are positively used to form monodispersed nanoparticles and composite

nanoparticles like core-shell type have been conducted. The laser ablation in nanoparticle research is regarded as the promising method at present which is possible to fabricate a novel function device in the area of electricity, semiconductor, energy and so on.

We have known PLD as a process during which a solid target is vaporized with laser irradiation, and then the nanoparticle formation in the gas phase is occurred, followed by its soft-landing on a substrate. But each process remains unclear to us. In order to apply the laser ablation method for the fabrication of functional materials, it is important to understand each step of the process so that we can put them to practical use. In this chapter, we divide the formation process of nanoparticle films as following steps for further studies: (1) temperature increase of solid surface by laser irradiation, (2) evaporation of the surface and its conversion to kinetic energy, (3) plume expansion with shock wave propagation, (4) supercooling of evaporated gas, (5) uniform sized nanoparticle formation, and (6) nanoparticle deposition and self-ordering on the substrate.

2. The formation process of nanoparticles by laser ablation

2.1 Laser irradiation analysis

The process of laser ablation commences from the interaction of lights and solids. When a laser irradiates on the surface of a solid target, the electromagnetic energy of the laser beam firstly turns into the excitation energy of electron, although the process may vary depending on the thermodynamic state of the solid. The energy conversion in the solid from the electronic excitation to the lattice vibration completes within some picoseconds. If the laser has nanosecond pulse, therefore, it is not necessary to take into consideration the non-equilibrium of the laser irradiation. Then, when viewed as a one-dimensional problem in the depth direction, the solid temperature can be described as the usual one-dimensional unsteady-state heat conduction Equation [7].

$$\frac{\partial T}{\partial t} = \frac{\partial}{\partial x}\left(\kappa \frac{\partial T}{\partial x}\right) + \frac{\alpha}{c_p \rho} I(x,t) \tag{1}$$

in the above equation, T stands for temperature, while κ for thermal conductivity, α for optical absorption coefficient, c_p for the specific heat, ρ for the density of the target material, and I for the value of laser energy, according to Lambert's law, along the depth direction after deduction of the loss caused by surface reflection.

On the other hand, a boundary condition is applied on the surface of target, where quantity of heat is removed from the surface corresponding to the heat of melting and evaporation. In addition, since the physical properties such as thermal conductivity are generally different between the solid and liquid phases, the equation should be applied separately in each phase [8].

As will be discussed in the next section, since the evaporating atoms during laser ablation are highly directional, the one-directional analysis is effective in most cases. However, in a certain case, one-dimensional analysis fails to take into consideration some factors, such as the thermal conductivity in radial direction which becomes dominant factor when the laser irradiation time becomes longer. Formerly, Houle and Hinsberg [9] applies a two-dimensional axisymmetric model with probabilistic algorithms to the analysis of laser ablation. This allows phenomena with different characteristic time such as absorption, melting, evaporation, and thermal conduction to be analyzed at the same time marching [10].

2.2 Knudsen layer

If the vapor pressure on the surface of the solids during evaporation is equal to the ambient pressure, the Maxwell velocity distribution for both evaporating and recondensing gas takes half shape of the distribution f^+ or f^-, being opposite in sign to each other, and the average value of velocity for these gases ought to be zero. In other words, if we consider the gases evaporating from the target surface and recondensing into it as a mixed gas, it is in an equilibrium state in terms of translational motion. However, when evaporation occurs drastically, as in the case of laser ablation, the balance of velocity distribution breaks down and a one-sided distribution appears for the evaporating gas, while the recondensing gas becomes remarkably little [11] so as to take the following velocity distribution [12].

$$f_s^+ \propto \exp\left[-\frac{2E_I + m\left(v_x^2 + v_y^2 + v_z^2\right)}{2kT_s}\right]; \tag{2}$$

$$v_x \gg 0, -\infty < v_y, v_z < \infty,$$

where direction x is normal to the target surface, directions y and z are in parallel to the surface, as an index of kinetic velocity v. While E_I is the accessible internal energy, T_s is the surface temperature, m is the atomic mass and k is Boltzmann constant. The movement of the evaporating atoms in vacuum and atmosphere is shown in **Figure 1** [13], by way of comparison. In vacuum as **Figure 1(a)**, the flow velocity as a macroscopic fluid is zero, while the kinetic velocity of individual atoms which are without interferences from the other atoms to form a whole gas flow (free molecular flow) is very high. When the gas density becomes high, as shown in **Figure 1(b)**, the velocity vector of atoms which keeps positive direction near the surface, gradually changes to negative direction with increasing distance from the surface due to the presence of recondesing atoms.

Meanwhile, the atomic velocity transits to the fluid velocity and the overall gas flow velocity increases. Thus, the velocity distribution of the evaporating atoms is relaxed in a very thin layer near the solid surface and finally reaches a shifted Maxwell equilibrium distribution as following [12]:

$$f_K^{\pm} \propto \exp\left[-\frac{2E_I + m\left\{\left(v_x - u_K\right)^2 + v_y^2 + v_z^2\right\}}{2kT_K}\right]; \tag{3}$$

$$-\infty < v_x, v_y, v_z < \infty,$$

where u is flow velocity and index K represents the state value at the very thin layer, which has a thickness corresponding to several mean free path and is called the Knudsen layer.

At the boundary of the Knudsen layer, the velocity of the gas u_K is equal to the speed of sound a_K, and the subsequent flow state will be determined by the temperature of the target surface, the type of ambient gas and its pressure [12, 14]. By solving the Boltzmann equation for the Knudsen layer, the velocity and angular directional distributions of evaporating gas near the solid surface have also been analyzed [15, 16].

2.3 Plume expansion and shock wave propagation

The configuration of plume (vapor atomic mass) formed by the vapor atoms emitted from the laser-irradiated area and shock wave formed by the piston effect

of the plume is shown in **Figure 2** [17]. From the laser irradiation zone shown in the leftmost part of the figure, since the vapor atoms emerge from the Knudsen layer in a certain angular distribution of velocity, the plume spreads out to the lateral

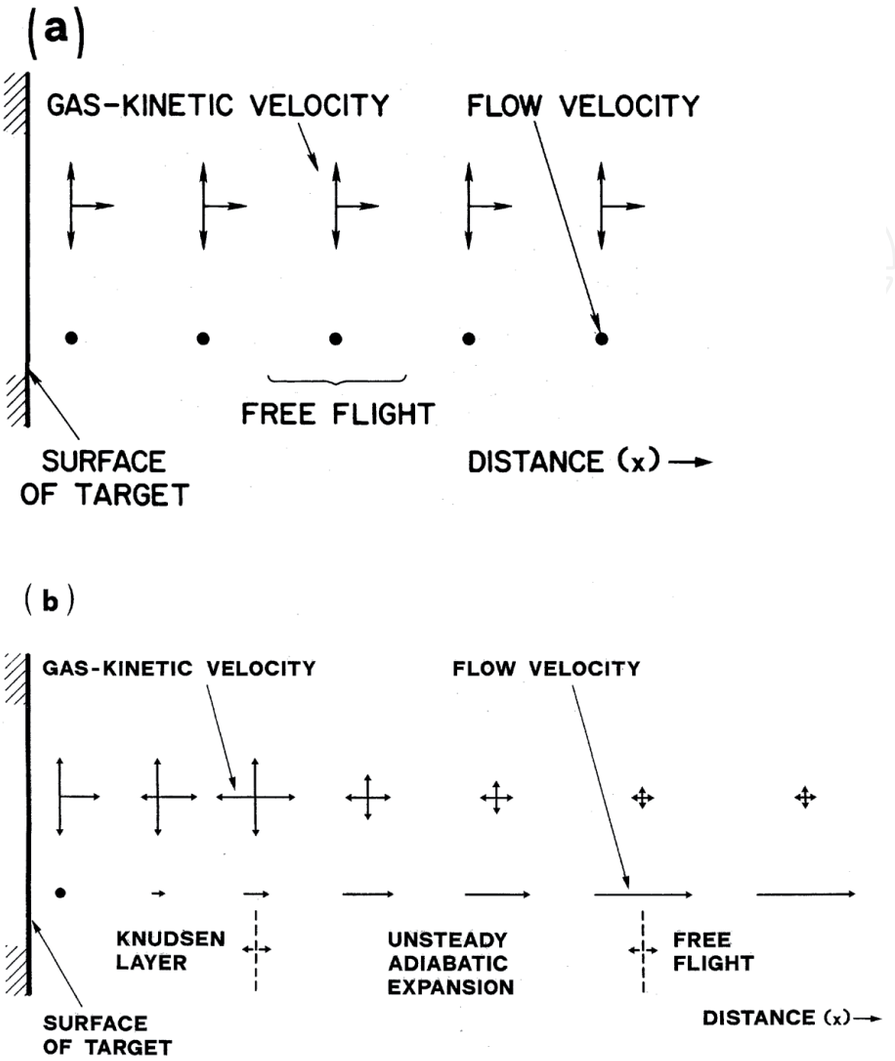

Figure 1.
(a) Schematic of representation of vapor atoms emitted from a target surface which enter immediately into free flight, in the case of evaporation in vacuum. (b) Schematic representation of Knudsen layer formation followed by an unsteady adiabatic expansion and free fight, in the case of evaporation in high density regime [13].

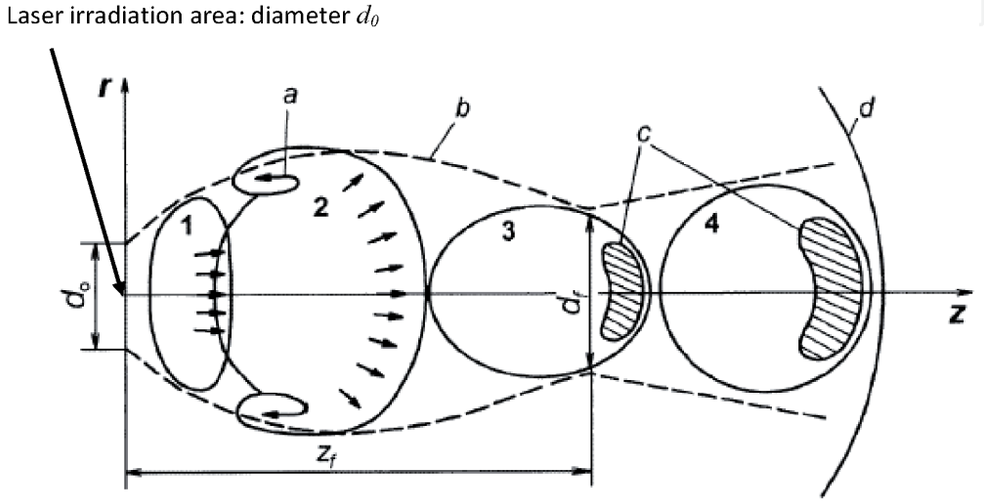

Figure 2.
Schematic drawing of laser plume expansion from the viewpoint of high-speed hydrodynamics [17].

direction along the central axis. In general, under the conditions of laser ablation, the pressure of the plume developed from the target is extremely higher than the ambient pressure, which is the so-called under-expansion jet in term of high-speed fluid dynamics (region 1 in **Figure 2**). Thereafter, the plume continues to expand, then it overinflates and forms a mushroom-like vortex (region 2 in **Figure 2**). The pressure of the overinflating plume becomes negative in comparison to the surrounding gas, which causes the plume to contract, resulting in a minimum diameter of the plume (region 3 in **Figure 2**). After this, the plume expands again and gradually decays (region 4 in **Figure 2**). At this stage, the resistance of the ambient gas is strong for the progress of the plume. The ambient gas atoms diffuse into the plume's front edge (hatched area in **Figure 2**) and form a diffusion region there. Since radicals of vapor atoms are generated in this diffusion region and plunge in collisional relaxations with the ambient gas atoms, luminescence can be likely observed in the region.

Since the atoms fall on a substrate from the luminescence zone, photogenic property in this zone would have a powerful effect on the characteristics of the film produced by laser ablation. The phenomenon has been analyzed through direct imaging by Intensified Charge Coupled Device (ICCD) and Laser Induced Fluorescence (LIF) [18–23]. The formation of nanoparticles is also thought to occur in this region [24].

2.4 Formation of nanoparticles

As described in the previous section, the formation process of the nanoparticle is highly related to the thermodynamic state in the dilution zone of the vapor atoms and ambient gas atoms. Hagena and Obert [25] conducted experiments using a supersonic nozzle to summarize the relationship between the size of atomic nanoparticles and the thermodynamic state as similitude rules in which parameters of molecular movement such as an interatomic potential are primary variables. Thus, estimating the equilibrium concentration of a nanoparticle from the thermodynamic conditions of the surrounding environment is useful for practical purposes and has been discussed in many publications. The rate constant for the nanoparticle equilibrium concentration is essentially based on the assumptions of statistical mechanics and is expressed as follows [26].

$$K_g = \frac{Q_t Q_r Q_v}{(q_t)^g} \exp\left(-\frac{E_g}{kT}\right) \tag{4}$$

Here, K_g is the rate constant of the equilibrium concentration in a nanoparticle consisted of atoms of the number g, while Q is the partition function of the nanoparticle with the subscripts t, r and v representing the translation, rotation and oscillation respectively. The variable q stands for the partition function of a mono-atom, E_g for the formation energy of the nanoparticle, k for the Boltzmann's constant, and T for the temperature of the system. The above equation describes the process in which the translational kinetic energy of a mono-atom transformed into the internal energy of the nanoparticle when it is captured by the nanoparticle. But there does not seem to be any detailed descriptions of this process in the classical theory of nanoparticle formation.

On the other hand, Eq. (4) refers to the nanoparticle concentration based on the steady-state theory. Generally speaking, the length of time it takes to form nanoparticle is not considered in this equation. However, for high-speed phenomena such as laser ablation, it is necessary to estimate the nanoparticle formation time to determine if the balance between condensation and evaporation on the surface of

nanoparticle is kept or not. If we are assuming that the velocity of vapor atoms is represented in the equilibrium Maxwell distribution, we can estimate the approximate nanoparticle formation time τ with the following equation.

$$\tau = \frac{\rho_c r\sqrt{2\pi kT}}{p\sqrt{m}} \tag{5}$$

In this equation, ρ_c stands for the internal density of the nanoparticle, while r the radius of the nanoparticle, p the vapor pressure, and m the mass of the vapor atoms. In order to obtain an exact solution, Gillespie [27] analyzed the process of nanoparticle formation as a random walk problem. However, no matter how rigorous the probabilistic analysis is, it is still based on classical nucleation theory. To address the problem related to the formation of nanometer-sized particle in non-equilibrium, the following issues should be considered.

a. The nucleation rate equation based on steady-state theory is valid only when the formation time of a critical nucleus is sufficiently short compared to the representative time of the system.

b. The classical theory is an available model at the range of relatively low supersaturation. In the case of high supersaturation, the internal degrees of freedom of the nanoparticle must be taken into an account, because differences are created among translational, rotational and vibrational temperature.

c. In spite of small systems, macroscopic physical properties and coefficients such as surface free energy, evaporation enthalpy, and condensation coefficient besides macroscopic concepts such as the Thomson–Gibbs formula are used. We have to correct these values and formula in conformity with the extent of non-equilibrium.

In recent years, with the development of computers, molecular dynamics or Direct Simulation Monte Carlo analyses which take into consideration the internal degrees of freedom of nanoparticles have been made [28], through which the Gibbs free energy and nanoparticle concentrations are elucidated under more realistic conditions.

3. Films fabricated by monodispersed nanoparticle beams

3.1 Monodispersed nanoparticle by size classification

In general, the size distribution of nanoparticles $f_x(x)$ growing in vapor phase is known to be described as the log-geometric distribution as follow [29].

$$f_X(x) = \frac{1}{x\sqrt{2\pi}\ln\sigma_g}\exp\left[-\frac{1}{2}\left(\frac{\ln\left(x/m_g\right)}{\ln\sigma_g}\right)^2\right] \quad x \geq 0 \tag{6}$$

Here m_g is the geometric mean and σ_g is the geometric standard deviation. A model has been proposed to explain the log-geometric distribution by assuming that the growth formula of a nanoparticle follows a certain Equation [30, 31]. It has also been experimentally confirmed that the size distribution of nanoparticles generated by laser ablation is log-geometric [32].

While sizes of nanoparticles have a certain distribution, the physical property of the nanoparticle may vary dramatically depending on its size. Thus, the sizes of nanoparticles should be in uniform when we need deal with them as macroscopic materials like nanoparticle films. Hence, in the early 2000s, some kinds of device to make the nanoparticle size in uniform has been actively invented and designed.

In those times, the size selection of aerosol particles is generally done in an electric field by deflecting charged particles generated from a source of the outbreaks such as combustion gas in Diesel engine. Afterward, the Differential Mobility Analyzer (DMA), as shown in **Figure 3** [33], which has been used to measure aerosol particles in the atmosphere, has been improved to the desired extent for applying on nanoparticles [34–36]. It is able to measure the particle size distribution by using the natural law in which a flying charged nanoparticle would land on different locations according to the balance between the electric mobility and fluid resistance, being deflected by an electric field [37]. Camata et al. [38] used a DMA system to estimate the geometric standard deviation of silicon nanoparticles with an average particle diameter of 2.8 nm and got a number of the geometric standard deviation between 1.2 ~ 1.3. Suzuki et al. [39] used DMA system on silicon nanoparticles and obtained a result of an average particle diameter of 2.8 nm and a geometric standard deviation of 1.2. A consistent system from a source of nanoparticles to its sampler is shown in **Figure 4** [34]. The nanoparticles generated by laser ablation pass through the gas phase annealing system, where the particle morphologies are controlled, and move to DMA to be classified by its size, and finally reach the particle sampler and the measurement systems.

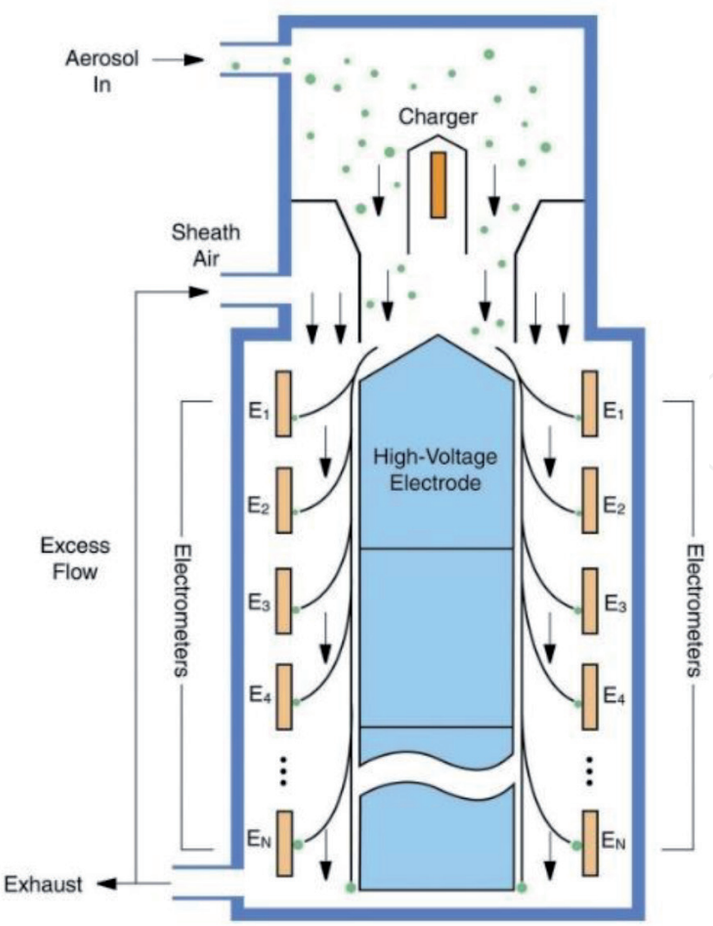

Figure 3.
Illustration of instrument capable of measuring size distributions of aerosol particles on basis of DMA [33].

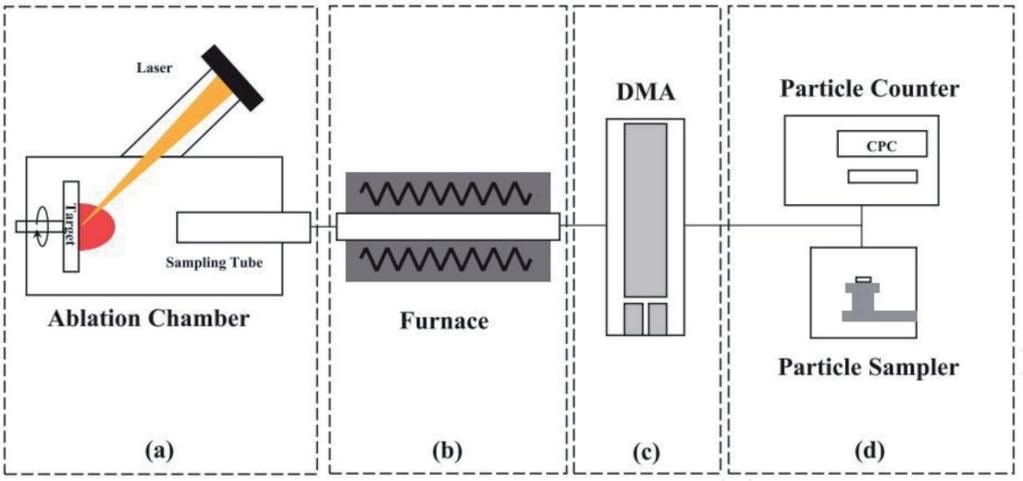

Figure 4.
Schematic of nanoparticle synthesis process using laser ablation, which is composed of (a) particle generator, (b) gas phase annealing, (c) particle classifying, and (d) particle measurement and correction [34].

Although the above methods require nanoparticles being charged in some way to select the size, the flank attack method proposed by Wu et al. [40] can be used for neutral nanoparticles. In this method, the nanoparticle beam is intersected with the atomic beams of inert gas such as argon or neon, and the nanoparticle can be sorted out in accordance with the size following the law in which the smaller the nanoparticle size, the greater the deflection angle of the beam.

3.2 The direct fabrication of monodisperse nanoparticles

In the previous section, the relationship between the growth rate and the size distribution of nanoparticles has been discussed. By understanding the growth process of nanoparticles, it is possible to control their size distribution. Laser Vaporization with Controlled Condensation (LVCC), as shown in **Figure 5** [41], is a method to control the average size of the nanoparticles by adjusting the conditions about nucleation and growth. By raising the temperature of the lower wall in ablation chamber with a heater and cooling down the upper wall with liquid nitrogen, the temperature gradient would cause the convection of ambient gas. When the vapor created by laser ablation drifts upward by the convection, the vapor becomes supersaturated near the upper cold wall, which results in nucleation

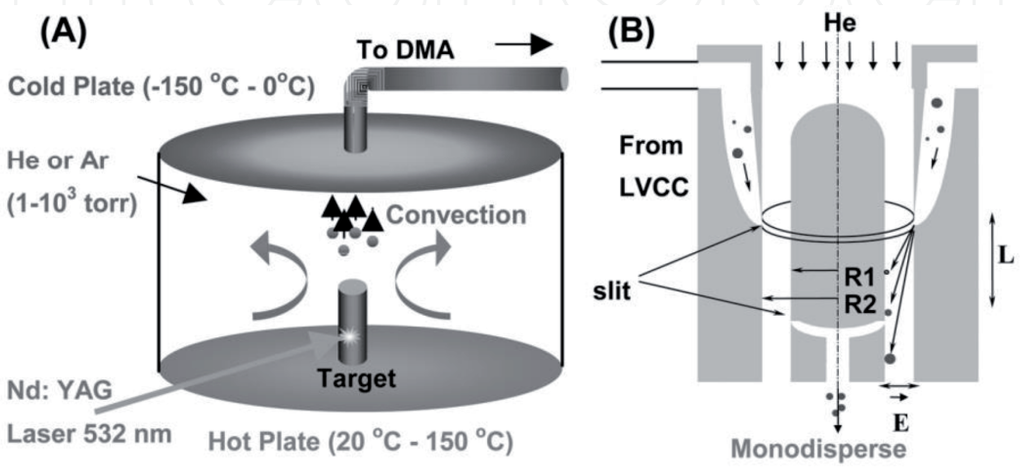

Figure 5.
(A) Experimental set-up for the synthesis of nanoparticles using the LVCC method. (B) Experimental setup for the LVCC method coupled with a DMA [41].

and condensation followed by nanoparticle forming. It is found that the higher the supersaturation is, that is, the larger the temperature gradient is, the smaller the average size of the nanoparticles becomes. Therefore, by adjusting the temperature gradient proficiently, it is possible to control the nanoparticle size. Furthermore, by combining LVCC and DMA, to control the average diameter and size distribution of nanoparticles would be possible.

In order to determine the size distribution by directly adjusting the growth process of the nanoparticles, it is necessary to control not only statically the degree of supersaturation but also dynamically its temporal variation of it. That is, it is necessary to rapidly increase the supersaturation level to complete the nucleation within a short period of time and to inhibit the subsequent nanoparticle growth in some ways [42].

As described in Section 2.3, a shock wave is generated in front of the plume by laser ablation. It is possible to use the shock wave to rapidly change the state quantity in the plume and increase the supersaturation at a fast rate. One example is the laser ablation process done in a closed space such as an ellipsoidal cell, in which the collision between the reflected shock wave and the plume front triggers the formation of nanoparticles instantly in a small area [43, 44]. The equipment fabricating monodispersed nanoparticles by using this phenomenon is called Spatiotemporal Confined Nanoparticle Source (SCCS), which is illustrated in **Figure 6** [45], as the fabrication process is restrained in the confined space and time.

3.3 Application of self-ordered nanoparticle films on substrate

The possibility of developing new functional materials with nanoparticle films has been pointed out for a long time [46], and many attempts have been made mainly to create light-emitting devices using the visible light emission from silicon

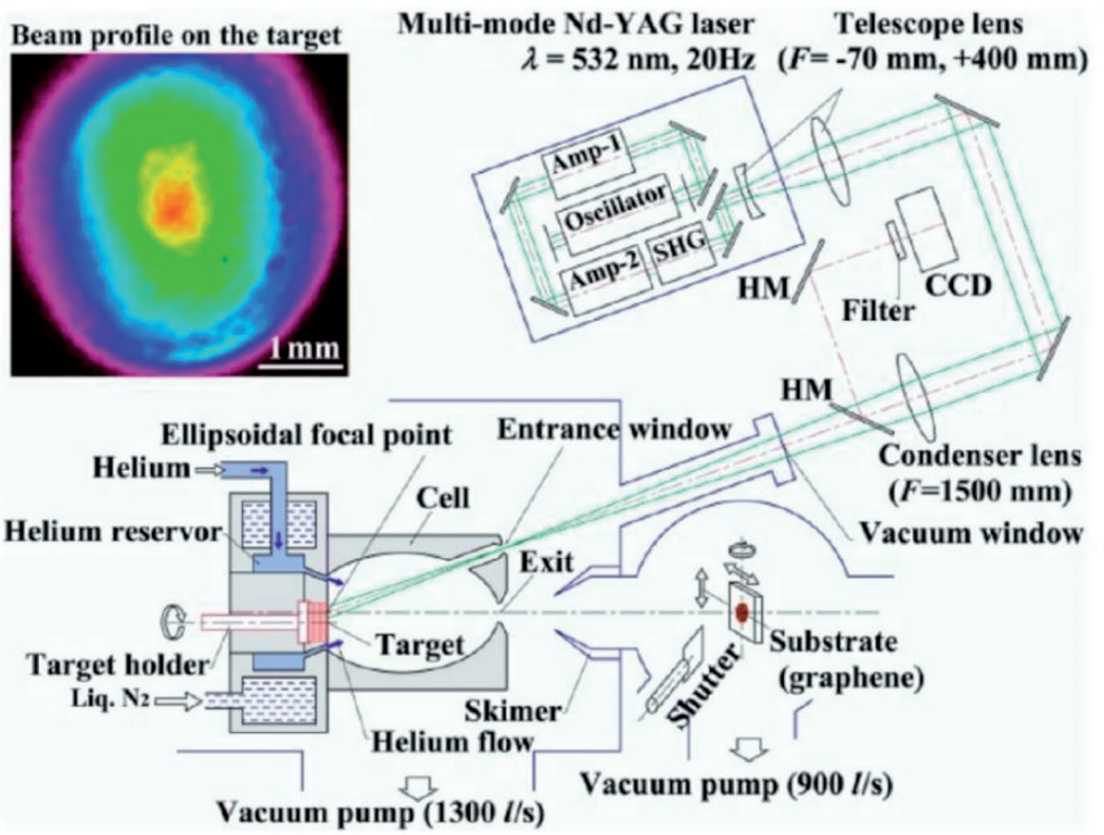

Figure 6.
Schematic view of new laser ablation-type silicon cluster beam system named SCCS [45].

nanoparticles [47–51]. Chen et al. [52] accumulated silicon nanoparticles on a substrate in an argon and oxygen atmosphere and researched on the effects of the gas pressure and annealing way on photoluminescence (PL). As a result, it was concluded that the emission band of 1.8–2.1 eV obtained from the experiments is based on the quantum effect since the blueshift of the emission varies depending on the nanoparticle size. Also, by accumulating silicon nanoparticles on a substrate in helium gas atmosphere, Kabashin et al. [53] found out that the microstructure on the nanoparticle film's surface varied depending on the helium gas pressure. When the helium gas pressure is higher than 1.5 Torr, it becomes a shape of porous film. Furthermore, it is concluded that the morphology of microstructure on the film surface determines the extent to which the natural oxidation of silicon nanoparticle affects PL luminescence.

In addition, the nanoparticle properties of iron oxide [54] and cobalt oxide [55] are studied for applying to a new functional device and material such as magnetic recording media, magnetic fluids and gas sensors. The properties of tungsten oxide nanoparticles [56] have been under research for being used as photocatalysts. However, while these applications of nanoparticles are still in the experimental stage, monodispersed nanoparticle beams are expected to improve the accuracy of these experiments.

On the other hand, from before, some studies focused attention on the function of laser irradiation to create an ordering of nanoparticles and investigated the influences of the intense and direction of electric field on the ordering appearance of nanoparticles. The phenomenon was called by Laser-Induced Periodic Surface Structures (LIPSS) [57, 58], which have led to a growing interest on how to build a new order of the nanoparticle array, as represented by the image of **Figure 7**. And Han et al. [59] confirmed by experiments and simulations that low-energy nanoparticle beams are effective in producing films of small nanoparticles with a wide range of sizes. Moreover, since the formation of ordered array is essential for making larger films, the technology of forming ordered nanoparticles by irradiating the substrate's surface with the beam of monodispersed nanoparticles which have a stable crystal structure has been expected. It is verified that the silicon nanoparticles fabricated by this technology spontaneously form a nanostructure ordering, and the formation

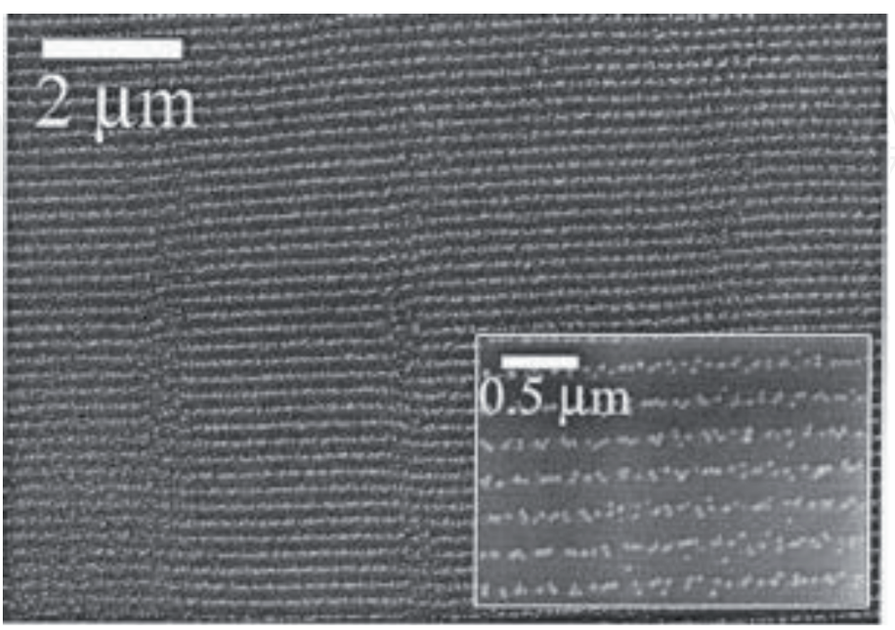

Figure 7.
SEM image of silicon nanoparticles produced by PLD and their long-range ordering controlled by subsequent laser irradiation [57].

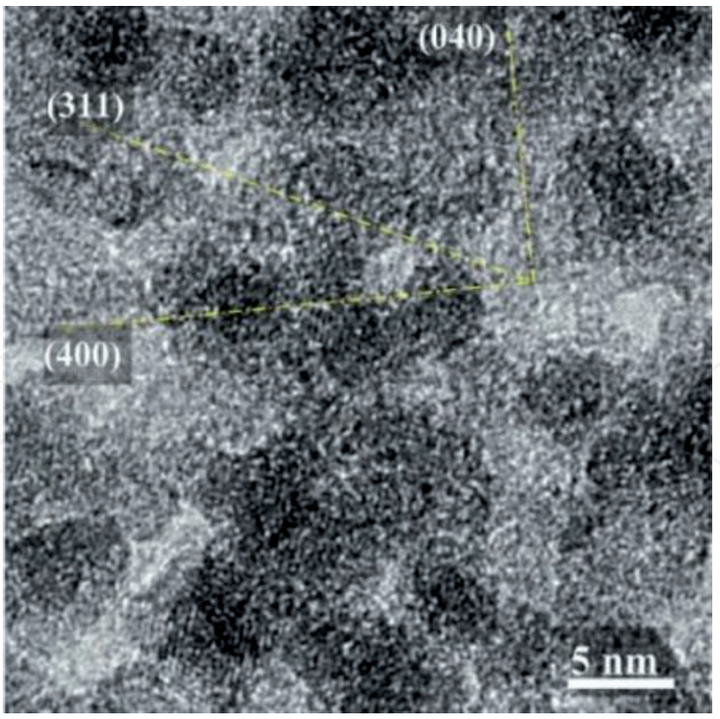

Figure 8.
HRTEM image of silicon cluster superlattice structures obtained with the use of the new laser ablation-type silicon cluster beam system [45].

mechanism has been studied [60]. The components of this structure are called silicon nanoblocks [61], which are expected to be applied on next-generation devices such as accumulator integration system with a solar cell [62], ultra-thin supercapacitor [63] and superlattice structures [45]. The silicon clusters possesing atomic crystalline structures generated by SCCS are depositing on the graphene substrate and forming shapes of silicon superlattice as shown in **Figure 8**.

In addition, it is found that interparticle spacing and pattern are the important parameters for characterizing the film consisting of nanoparticle array. We can extract the useful properties from the nanoparticle films, depending on the interparticle spacing range of electron tunneling, optical near field or spin exchange interaction. In the next generation of laser ablation, it seems to be one of critical challenges to clarify and control the ordering of nanoparticles based on the viewpoint of the interparticle spacing.

4. Summary

To apply the nanostructured particle films on new functional materials, it is important to study the formation process. Therefore, in this chapter, we stared from the mechanism of laser ablation process and then found that monodispersed nanoparticle beams are necessary for fabricating nanoparticle films and that, when used as a macroscopic material, the technology based on the self-ordering of nanoparticles is essential to make large films. It is expected to control the interparticle spacing and its pattern of nanoparticle structure in the films to obtain new and useful properties which are potentially underlying in the films as functional devices. In order to realize such devices, laser ablation remains a promising technology for the future, and worth studied for more possibilities.

Author details

Toshio Takiya[1,2*] and Naoaki Fukuda[1,3]

1 Hitachi Zosen Corporation, Osaka, Japan

2 Hitz Collaborative Research Institute, Osaka University, Osaka, Japan

3 Research Center for the 21st Century, Osaka Prefecture University, Osaka, Japan

*Address all correspondence to: takiya@hitachizosen.co.jp

References

[1] H. W. Kroto, J. R. Heath, S. C. O'Brien, R. F. Curl and R. E. Smalley, C60: Buckminsterfullerene, Nature, vol. 318, p.62-163 (1985)

[2] W. T. Nichols, G. Malyavanatham, D. E. Henneke, D. T. O'Brien, M. F. Becker and J. W. Keto, Bimodal Nanoparticle Size Distributions Produced by Laser Ablation of Microparticles in Aerosols, Journal of Nanoparticle Research, vol.4, p.423-432(2002)

[3] A. E. Mayer and A. A. Ebel, Shock-induced compaction of nanoparticle layers into nanostructured coating, J. Appl. Phys. 122, 165901 (2017)

[4] T. Takiya, N. Fukuda, N. Inoue, M. Han, M. Yaga and Y. Iwata, Dynamics of the Shock Wave Accompanied by Nanoparticle Formation in the PLA Processes, Adv. Studies Theor. Phys., vol.4-7, 305-316(2010)

[5] E. Ueno, N. Fukuda, H. Fukuoka, M. Yaga, I. Umezu, M. Han and T. Takiya, Nanoparticle formation by interaction between laser ablated plume and shock waves, 17th International Symposium on Small Particles and Inorganic Clusters, (2014)

[6] A. Higo, K. Katayama, H. Fukuoka, T. Yoshida, T. Aoki, M. Yaga and I. Umezu, Expansion of laser-induced plume after the passage of a counter shock wave through a background gas, Appl. Phys. A, vol.126, Article number: 304 (2020)

[7] A. Vertes, R. W. Dreyfus and D. E. Platt, Modeling the thermal-to-plasma transitions for Cu photoablation, IBM J. Res. Develop. 38-1, 4-10(1994)

[8] A. Peterlongo, A. Miotello and R. Kelly, Laser-pulse sputtering of aluminum: Vaporization, boiling, superheating, and gas-dynamic effects, Phys. Rev. E 50-6, 4716-4727(1994)

[9] F.A. Houle and W.D. Hinsberg, Stochastic simulation of heat flow with application to laser–solid interactions, Appl. Phys. A, vol.66, p.143-151(1998)

[10] M. Han, S. Kiyama, M. Muto, A. Fukuda, T. Sawada and Y. Iwata, Cluster formation dynamics in a locally-confined gas layer mixed with the plume ablated by pulsed laser irradiation, Nucl. Instr. Meth. Phys. Res., B153, 302-308(1999)

[11] S. I. Anisimov, Vaporization of Metal Absorbing Laser Radiation, J. Exp. Theor. Phys., 27-1, 182-183(1968)

[12] R. Kelly, On the dual role of the Knudsen layer and unsteady, adiabatic expansion in pulse sputtering phenomena, J. Chem. Phys. 92-8, 5047-5056(1990)

[13] R. Kelly, A. Miotello, A. Mele, A. G. Guidoni, J. W. Hastie, P. K. Schenck and H. Okabe, Gas-dynamic effects in the laser-pulse sputtering of AlN: is there evidence for phase explosion?, Appl. Surf. Sci., vol.133-4, p.251-269(1998)

[14] C. J. Knight, Theoretical Modeling of Rapid Surface Vaporization with Back Pressure, AIAA J, 17-5, 519-523(1979)

[15] L. V. Zhigilei and B. J. Garrison, Velocity distributions of molecules ejected in laser ablation, Appl. Phys. Lett. 71-4, 551-553(1997)

[16] A. V. Gusarov and I. Smurov, Target-vapour interaction and atomic collisions in pulsed laser ablation, J. Phys. D: Appl. Phys. 34, 1147-1156(2001)

[17] A. V. Bulgakov and N. M. Bulgakova, Gas-dynamic effects of the interaction between a pulsed laser-ablation plume and the ambient gas: analogy with an underexpanded jet, J. Phys. D: Appl. Phys. 31, 693-703(1998)

[18] S. S. Harilal, C. V. Bindhu, M. S. Tillack, F. Najmabadi and A. C. Gaeris,

Plume splitting and sharpening in laser-produced aluminium plasma, J. Phys. D: Appl. Phys. 35, 2935-2938(2002)

[19] I. Umezu, M. Inada, K. Kohno, T. Yamaguchi, T. Makino and A. Sugimura, Reaction between nitrogen gas and silicon species during pulsed laser ablation, J. Vac. Sci. Technol. A 21-5, 1680-1682(2003)

[20] Y. Nakata, G. Soumagne, T. Okada, M. Maeda, Pulsed-laser deposition of barium titanate films and plume dynamics, Appl. Surf. Sci., p.127-129, 650-654(1998)

[21] D. B. Geohegan, Fast intensified-CCD photography of YBa2Cu3O7−x laser ablation in vacuum and ambient oxygen, Appl. Phys. Lett. 60-22, 2732-2734(1992)

[22] D. B. Geohegan, A. A. Puretzky, G. Duscher and S. J. Pennycook, Time-resolved imaging of gas phase nanoparticle synthesis by laser ablation, Appl. Phys. Lett. 72-23, 2987-2989(1998)

[23] D. B. Geohegan, A. A. Puretzky, G. Duscher and S. J. Pennycook, Photoluminescence from gas-suspended SiOx nanoparticles synthesized by laser ablation, Appl. Phys. Lett. 73-4, 438-440(1998)

[24] M. Han, Y. Gong, J. Zhou, C. Yin, F. Song, N. Muto, T. Takiya and Y. Iwata, Plume dynamics during film and nanoparticles deposition by pulsed laser ablation, Phys. Lett. A302, 182-189(2002)

[25] O. F. Hagena and W. Obert, Cluster Formation in Expanding Supersonic Jets: Effect of Pressure, Temperature, Nozzle Size, and Test Gas, J. Chem. Phys. 56-5, 1793-1802(1972)

[26] for example, D. J. McGinty, Molecular dynamics studies of the properties of small clusters of argon atoms, J. Chem. Phys. 58-11, 4733-4742(1973)

[27] D. T. Gillespie, A stochastic analysis of the homogeneous nucleation of vapor condensation, J. Chem. Phys. 74-1, 661-678(1981)

[28] for example: N. Bykov and Y. Gorbachev, Mechanics - Seventh Polyakhov's Reading, 2015 International Conference, St.-Petersburg, Russia, February (2015)

[29] L. Landström, Formation of Nanoparticles by Laser-Activated Processes, Comprehensive Summaries of Uppsala Dissertations from the Faculty of Science and Technology 855, p.10, Acta Universitatis Upsalensis, Uppsala, (2003)

[30] J. Söderlund, L. B. Kiss, G. A. Niklasson, and C. G. Granqvist, Lognormal Size Distributions in Particle Growth Processes without Coagulation, Phys. Rev. Lett. 80-11, 2386-2388 (1998)

[31] L. B. Kiss, J. Söderlund, G. A. Niklasson and C. G. Granqvist, New approach to the origin of lognormal size distributions of nanoparticles, Nanotechnology 10, 25-28 (1999)

[32] N. Koshizaki, A. Narazaki and T. Sasaki, Size distribution and growth mechanism of Co3O4 nanoparticles fabricated by pulsed laser deposition, Scripta mater. 44, 1925-1928 (2001)

[33] T. Johnson, R. Caldow, A. Pöcher, A. Mirme and D. Kittelson, An Engine Exhaust Particle Sizer Spectrometer for Transient Emission Particle Measurements, 7th ETH- ETH Conference on Combustion Generated Particles, Zürich, Switzerland (2003)

[34] M. Kim, S. Osone, T. Kim, H. Higashi and T. Seto, Synthesis of Nanoparticles by Laser Ablation: A Review, KONA Powder and Particle Journal No. 34 (2017)

[35] P. M. Denby and D. A. Eastham, Efficient technique for producing

high-brightness, size-selected cluster beams, Appl. Phys. Lett. 79-15, 2477-2479 (2001)

[36] E. Hontañón and F. E. Kruis, A Differential Mobility Analyzer (DMA) for Size Selection of Nanoparticles at High Flow Rates, Aeros. Sci. and Technol., vol.43-1, 25-37(2009)

[37] T. Seto, Y. Kawakami, N. Suzuki, M. Hirasawa, S. Kano, N. Aya, S. Sasaki and H. Shimura, Evaluation of Morphology and Size Distribution of Silicon and Titanium Oxide Nanoparticles Generated by Laser Ablation, J. Nanoparticle Res., vol.3, p.185-191 (2001)

[38] R. P. Camata, H. A. Atwater, K. J. Vahala and R. C. Flagan, Size classification of silicon nanocrystals, Appl. Phys. Lett. 68-22, 3162-3164 (1996)

[39] N. Suzuki, T. Makino, Y. Yamada, T. Yoshida and T. Seto, Monodispersed, nonagglomerated silicon nanocrystallites, Appl. Phys. Lett. 78-14, 2043-2045 (2001)

[40] H. P. Wu, A. Okano, K. Takayanagi, Photoluminescence properties of size-selected Si nanocluster films prepared by laser ablation, Appl. Phys. A 71-6, 643-646(2000)

[41] G. Glaspell, V. Abdelsayed, K. M. Saoud, and M. S. El-Shall, Vapor-phase synthesis of metallic and intermetallic nanoparticles and nanowires: Magnetic and catalytic properties, Pure Appl. Chem., vol. 78-9, pp.1667-1689(2006)

[42] S. Yamamuro, K. Sumiyama and K. Suzuki, Monodispersed Cr cluster formation by plasma-gas-condensation, J. Appl. Phys., 85-1, 483-489 (1999)

[43] Y. Iwata, M. Kishida, M. Muto, S. Yu, T. Sawada, A. Fukuda, T. Takiya, A. Komura and K. Nakajima, Chem. Phys. Lett. 358, 36-42(2002)

[44] Y. Iwata, M. Muto, T. Sawada, M. Han, A. Fukuda, S. Okayama, H. Matsuhata, H. Yamauchi, M. Kishida, T. Takiya, A. Komura and K. Nakajima, Well-defined Cluster Beam Deposition (CBD) Developed for Vacuum Synthesis of Nanostructures, Proc. 5th ISTC Scientific Advisory Committee Seminar, p.1-6, St Petersburg, Russia (2002)

[45] Y. Iwata, K. Tomita, T. Uchida and H. Matsuhata, Crystallographic Coalescence of Crystalline Silicon Clusters into Superlattice Structures, Cryst. Growth Des. 15-5, 2119-2128(2015), DOI: 10.1021/cg5016753

[46] G. D. Stein, DESIGN AND USE OF METAL CLUSTER BEAM SOURCES: IMPLICATIONS FOR THIN FILM DEVICES, Proc. Int. Ion Eng. Cong., ISIAT'83 & IPAT'83, Kyoto, 1165-1176B (1983)

[47] S. Li, S. J. Silvers and M. S. El-Shall, Surface Oxidation and Luminescence Properties of Weblike Agglomeration of Silicon Nanocrystals Produced by a Laser Vaporization–Controlled Condensation Technique, J. Phys. Chem. B 101, 1794-1802 (1997)

[48] L. Patrone, D. Nelson, V.I. Safarov, S. Giorgio, M. Sentis & W. Marine, Synthesis and properties of Si and Ge nanoclusters produced by pulsed laser ablation, Appl. Phys. A69[Suppl.], S217-S221 (1999)

[49] F. Huisken, B. Kohn and V. Paillard, Structured films of light-emitting silicon nanoparticles produced by cluster beam deposition, Appl. Phys. Lett. 74-25, 3776-3778 (1999)

[50] L. Patrone, D. Nelson, V. I. Safarov, M. Sentis and W. Marine, Photoluminescence of silicon nanoclusters with reduced size dispersion produced by laser ablation, J. Appl. Phys. 87-8, 3829-3837 (2000), DOI: 10.1063/1.372421

[51] A. V. Kabashin and M. Meunier, Photoluminescence characterization of Si-based nanostructured films produced by pulsed laser ablation, J. Vac. Sci. Technol. B 19-6, 2217-2222 (2001), DOI: 10.1116/1.1420494

[52] X. Y. Chen, Y. F. Lu, Y. H. Wu, B. J. Cho, M. H. Liu, D. Y. Dai and W. D. Song, Mechanisms of photoluminescence from silicon nanocrystals formed by pulsed-laser deposition in argon and oxygen ambient, J. Appl. Phys. 93-10, 6311-6319(2003), DOI: 10.1063/1.1569033

[53] A. V. Kabashin, J.-P. Sylvestre, S. Patskovsky and M. Meunier, Correlation between photoluminescence properties and morphology of laser-ablated Si/SiOx nanostructured films, J. Appl. Phys. 91-5, 3248-3254(2002), DOI:10.1063/1.1446217

[54] L. Zbroniec, T. Sasaki, N. Koshizaki, Ambient gas effects on iron oxide particle aggregated films prepared by laser ablation, Scripta mater. 44, 8-9, 1869-1872(2001), DOI: 10.1016/S1359-6462(01)00735-7

[55] Q. Li, T. Sasaki and N. Koshizaki, Pressure dependence of the morphology and size of cobalt (II,III) oxide nanoparticles prepared by pulsed-laser ablation, Appl. Phys. A 69, 115-118(1999), DOI: 10.1007/s003390050982

[56] S. Li, M. S. El-Shall, Synthesis of nanoparticles by reactive laser vaporization: silicon nanocrystals in polymers and properties of gallium and tungsten oxides, Appl. Surf. Sci. 127-129, 330-338(1998), DOI: 10.1016/S0169-4332(97)00651-X

[57] J. D. Fowlkes, A. J. Pedraza, D. A. Blom and H. M. Meyer III, Surface microstructuring and long-range ordering of silicon nanoparticles, Appl. Phys. Lett. 80-20, 3799-3801(2002), DOI: 10.1063/1.1480106

[58] A. J. Pedraza, J. D. Fowlkes, D. A. Blom, H. M. Meyer, Laser-induced nanoparticle ordering, J. Mater. Res. 17-11, 2815-2822(2002), DOI: 10.1557/JMR.2002.0409

[59] Han Min, Wang Zhaoye, Chen Pingping, Yu Shengwen, Wang Guanghou, Mechanism of neutral cluster beam deposition, Nucl. Instr. Meth. Phys. Res. B135, 1-4, 564-569(1998), DOI: 10.1016/S0168-583X(97)00635-6

[60] M. Muto, M. Oki, Y. Iwata, H. Yamauchi, H. Matsuhata, S. Okayama, Y. Ikuhara, T. Iwamoto and T. Sawada, Silicon nanoparticle lattice system(CLS) formed on an amorphous carbon surface by supersonic nanoparticle beam irradiation, Proc. Int. Symp. On Atomic Nanoparticle Collisions, Saint-Peteraburg(2003)

[61] Y. Iwata, Silicon Nanoblocks Pave The Way for A New Conceptual Nanoarchitecture, AIST Today Vol. 3, No. 7, 4-6 (2003)

[62] Q. Rehman, A. D. Khan, M. Noman, H. Ali, A. Raufd and M. S. Ahmad, Super absorption of solar energy using a plasmonic nanoparticle based CdTe solar cell, RSC Advances, Issue 59, (2019), DOI: 10.1039/C9RA07782K

[63] M. Hassan, M. A. Gondal, E. Cevikc, T. F. Qahtan, A. Bozkurt, M. A. Dastageer, High performance pliable supercapacitor fabricated using activated carbon nanospheres intercalated into boron nitride nanoplates by pulsed laser ablation technique, Arabian J. Chem., vol.13-8, p.6696-6707(2020), DOI: 10.1016/j.arabjc.2020.06.024